BEÜ Fen Bilimleri Dergisi
8 (2), 628-641, 2019

BEU Journal of Science
8 (2), 628-641, 2019

Araştırma Makalesi / Research Article

Static Analysis of Orthotropic Euler-Bernoulli and Timoshenko Beams With Respect to Various Parameters

Mustafa Halûk SARAÇOĞLU*, Gökhan GÜÇLÜ, Fethullah USLU

Kütahya Dumlupınar University, Department of Civil Engineering, Kütahya
(ORCID:0000-0003-3842-5699) (ORCID:0000-0003-2931-9501) (ORCID:0000-0001-8057-5119)

Abstract
In this study, deflections of orthotropic beams along the beam length are calculated by using static analysis according to Euler-Bernoulli and Timoshenko beam theories. Since the mechanical properties of the materials change as the orientation angle of fibers changes, the formulation is carried out using the equivalent Young's modulus and the equivalent shear modulus. Orthotropic beams are modeled as isotropic beams by using equivalent moduli. Governing equations are derived. Two numerical examples with different orthotropic materials are given for different boundary and loading conditions. The effect of changing the orientation angle of the fibers on the deflection values is also considered. Orientation angle, material properties, length to depth ratio has been considered as parameters in the static analysis of orthotropic beams. Results are also compared with steel which is an isotropic material and presented in the form of tables and graphs which may be useful.

Keywords: Euler-Bernoulli Beam Theory, Timoshenko Beam Theory, Fiber Reinforced Composites, Equivalent Young's and Shear Moduli, Orthotropic Beams, Static Analysis.

Çeşitli Parametrelere Göre Ortotrop Euler-Bernoulli ve Timoshenko Kirişlerinin Statik Analizi

Öz
Bu çalışmada kiriş uzunluğu boyunca ortotrop kirişlerin çökmeleri Euler-Bernoulli ve Timoshenko kiriş teorilerine göre statik analiz yapılarak hesaplanmıştır. Malzemelerin mekanik özellikleri, liflerin oryantasyon açısına bağlı olarak değiştiği için, yönetici denklemlerin türetilmesi, eşdeğer elastisite modülü ve eşdeğer kayma modülü kullanılarak gerçekleştirilmiştir. Ortotrop kirişler eşdeğer modüller kullanılarak izotrop kirişler olarak modellenmiştir. Farklı ortotrop malzemelerden oluşan iki sayısal örnek farklı sınır koşulları ve yükleme durumları için verilmiştir. Liflerin oryantasyon açılarının değişiminin çökme değerlerine etkisi de ele alınmıştır. Ortotrop kirişlerin statik analizinde oryantasyon açısı, malzeme özellikleri, uzunluk-derinlik oranı parametreler olarak alınmıştır. Sonuçlar ayrıca izotrop olan çelik malzemesi ile karşılaştırılmış ve faydalı olabilecek tablo ve grafikler şeklinde sunulmuştur.

Anahtar kelimeler: Euler-Bernoulli Kiriş Teorisi, Timoshenko Kiriş Teorisi, Lifli Kompozitler, Eşdeğer Elastisite ve Kayma Modülleri, Ortotrop Kirişler, Statik Analiz.

1. Introduction

Areas of use of beams aren't limited to only structures. It also finds extensive use in different disciplines such as mechanical and space engineering. For instance aircraft wings, helicopter propellers, robot arms are also analysed as beam elements.

Many theories have been developed for the analysis of beams. Euler-Bernoulli beam theory (EBT) and Timoshenko beam theory (TBT) are the most prominent of these theories. In the literature it is possible to come across many studies on this subject.

*Sorumlu yazar: mhaluk.saracoglu@dpu.edu.tr
Geliş Tarihi: 11.12.2018, Kabul Tarihi: 29.04.2019

Labuschagne et al. [1] have compared three different models for the dynamic analysis of a cantilever beam. Reddy [2] rearranged classical and first order beam and plate theories by using Von Karman's nonlinear strains and Eringen's nonlocal differential constitutive relations. Sayyad [3] compared various improved beam theories for a simply supported thick isotropic beam in terms of bending and free vibration analysis. For a fixed beam loaded with uniformly distributed load; Aykanat [4] examined the behavior of the beam's strain and deformation by using nonlocal elasticity theory. Carrera and Giunta [5] proposed several axiomatic refined theories for the linear static analysis of isotropic beams. Elshafei [6] analysed isotropic and orthotropic beams using first order shear deformation theory and developed a finite element model. Whitney [7] analysed orthotropic beams under single loads according to the classical elasticity theory. With a new approach Li [8] investigated the static and dynamic behavior of Timoshenko and Euler-Bernoulli beams that have functionally graded material. De Rosa and Franciosi [9] applied the Mohr theory to the computation of displacements and rotations of carbon nanotubes, and they derive some formula which allows the direct generalization of the Mohr theory to the nonlocal Euler–Bernoulli and Timoshenko beam theories in their paper. Palmeri and Cicirello [10] analysed cracked beams under static loads and they offer a novel and physically-based modelling of slender Euler–Bernoulli beams and short Timoshenko beams with cracks, conducing in both cases to exact closed-form solutions. Saracoglu et al. [11] investigated orthotropic beams with different boundary conditions and different loads and also they modeled on computer analytically with Mathematica, Matlab software programs.

In this paper deflections of orthotropic beams along beam length are calculated by using static analysis according to EBT and TBT. Unlike other studies; while static analysis are performed orthotropic beams are modeled as isotropic beams. The formulations are derived by using equivalent Young's modulus and the equivalent shear modulus. The following materials which shows orthotropic character are studied: graphite-epoxy, glass-epoxy, boron-epoxy. Also steel which is an isotropic material is studied for comparison. As examples; simply supported beam with a uniformly distributed load and cantilever beam loaded by a vertical single load applied at the free tip are considered. Deflections are calculated for different orientation angles of the fibers.

2. Beam Theories

The most commonly used beam theory is EBT which is also called classical beam theory. In cases where the shear deformations cannot be neglected, TBT is widely used.

Positive load directions, coordinate system, displacements and parametric dimensions used in this study are given in Figure 1.

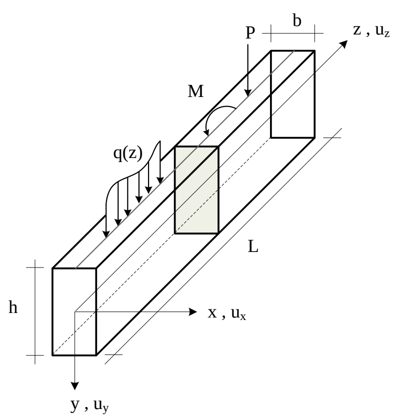

Figure 1. Beam geometry, coordinate system, displacements, dimensions

Orthotropic and composite materials have high strength, low weight and high rigidity. They are widely used in disciplines such as civil, mechanical and space engineering. For orthotropic and composite materials; the ratio of E/G is generally much greater than those of isotropic materials.

The developed beam models have made it possible to solve a large number of engineering problems. Figure 2 shows the displacement of a point on the beam and the shape of the plane cross-section after the deformations in EBT and TBT.

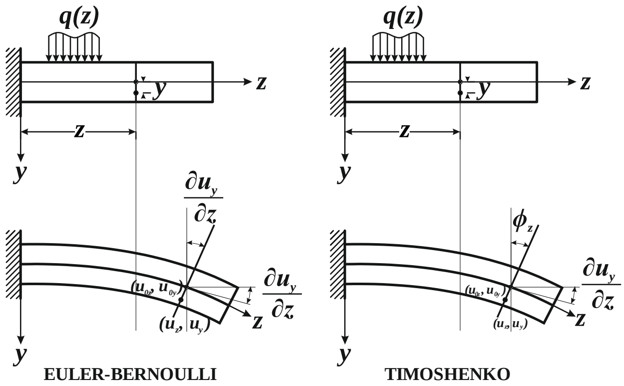

Figure 2. Displacement of a point and shape of the cross section after deformation

2.1. Euler-Bernoulli Beam Theory

This theory, first suggested in the 1700, was not accepted until the 19th century Eiffel tower and Ferris wheel constructions. The displacement of a selected point on the beam according to the EBT is as given in Figure 2.

The assumptions made by the EBT are; plane sections remain plane and normal to the axis of the beam after deformation.

Under these assumptions we can write

$$\varepsilon_{xx} = \frac{\partial}{\partial x} u_x = 0\,, \quad \varepsilon_{yy} = \frac{\partial}{\partial y} u_y = 0\,, \quad \gamma_{xy} = \frac{\partial}{\partial y} u_x + \frac{\partial}{\partial x} u_y = 0 \tag{1}$$

Functional expressions of displacements in Eq. (2) can be defined in the form of $u_x(x,y,z) = u_{x1}(z)$, $u_y(x,y,z) = u_{y1}(z)$ and $u_z(x,y,z) = u_{z1}(z)$ [12].

The displacement field of the EBT is;

$$\begin{aligned} u_x &= u_{x1} \\ u_z &= u_{z1} - y \frac{\partial}{\partial z} u_{y1} \\ u_y &= u_{y1} \end{aligned} \tag{2}$$

2.1. Timoshenko Beam Theory

The displacement of a selected point on the beam according to the TBT is shown in Figure 2. The basic assumptions for TBT are identical to EBT assumptions except for the second assumption of the EBT. Instead of that, in TBT; plane cross sections, will remain plane after deformation assumption is made [13]. This assumption differs from EBT which presumes that plane cross sections remains normal to the axis of the beam after deformation. For Timoshenko beams, plane cross sections will rotate due to shear forces. Accordingly, $\varepsilon_{zz}, \gamma_{xz}$ and γ_{zy} strains are non-zero and must be calculated.

Displacements for TBT can be given as in Eq. (3)

$$\begin{aligned} u_x(x,y,z) &= u_{x1}(z) \\ u_z(x,y,z) &= u_{z1}(z) - x\phi_y(z) + y\phi_x(z) \\ u_y(x,y,z) &= u_{y1}(z) \end{aligned} \tag{3}$$

Here ϕ_x and ϕ_y denotes the angles of rotation relative to *x* and *y* axes respectively. Their mathematical expressions are,

$$\phi_x = -\frac{\partial}{\partial z} u_{y1} \ , \qquad \phi_y = \frac{\partial}{\partial z} u_{x1} \tag{4}$$

2.3. Equivalent Moduli

The material constants to be used for the static analysis of orthotropic beams are not the same as isotropic ones. For fiber-reinforced orthotropic materials, the constants can be converted to an equivalent modulus using the orientation angle of the fibers.

The angle between the beam axis and the fiber axis called orientation angle (θ); is shown in Figure 3.

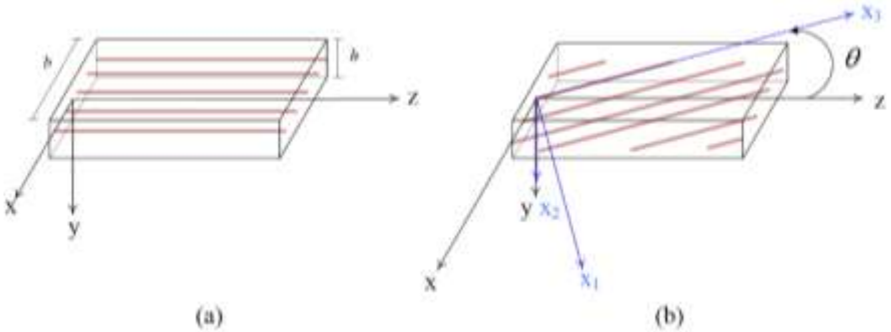

Figure 3. Orientation angle of fibers; a) 0 degree, b) θ degree

2.3.1. Equivalent Young's modulus

The equivalent Young's modulus of a fiber reinforced orthotropic element can be defined as in Eq. (5) depending on the material properties [14].

$$E_{eq} = \frac{12}{h^3 D_{11}^*} \tag{5}$$

where

$$D_{11}^* = \frac{\left(D_{22}D_{66} - D_{26}D_{26}\right)}{\left(D_{11}\left(D_{22}D_{66} - D_{26}D_{26}\right) + D_{12}\left(D_{16}D_{26} - D_{12}D_{66}\right) + D_{16}\left(D_{12}D_{26} - D_{22}D_{16}\right)\right)} \tag{6}$$

here D_{ij} are calculated according to the material properties and the direction of the fibers.

$$
\begin{aligned}
&D_{ij} = \frac{h^3}{12}\,\overline{Q}_{ij} \\
&\overline{Q}_{11} = Q_{11}\cos^4\theta + 2(Q_{12} + 2Q_{66})\sin^2\theta\cos^2\theta + Q_{22}\sin^4\theta \\
&\overline{Q}_{12} = (Q_{11} + Q_{22} - 4Q_{66})\sin^2\theta\cos^2\theta + Q_{12}(\sin^4\theta + \cos^4\theta) \\
&\overline{Q}_{22} = Q_{11}\sin^4\theta + 2(Q_{12} + 2Q_{66})\sin^2\theta\cos^2\theta + Q_{22}\cos^4\theta \\
&\overline{Q}_{16} = (Q_{11} - Q_{12} - 2Q_{66})\sin\theta\cos^3\theta + (Q_{12} - Q_{22} + 2Q_{66})\sin^3\theta\cos\theta \\
&\overline{Q}_{26} = (Q_{11} - Q_{12} - 2Q_{66})\sin^3\theta\cos\theta + (Q_{12} - Q_{22} + 2Q_{66})\sin\theta\cos^3\theta \\
&\overline{Q}_{66} = (Q_{11} + Q_{22} - 2Q_{12} - 2Q_{66})\sin^2\theta\cos^2\theta + Q_{66}(\sin^4\theta + \cos^4\theta) \\
&Q_{11} = \frac{E_1}{1-\upsilon_{12}\upsilon_{21}}, \quad Q_{12} = \frac{\upsilon_{12}E_2}{1-\upsilon_{12}\upsilon_{21}} = \frac{\upsilon_{21}E_1}{1-\upsilon_{12}\upsilon_{21}}, \quad Q_{22} = \frac{E_2}{1-\upsilon_{12}\upsilon_{21}}, \quad Q_{66} = G_{12}
\end{aligned} \tag{7}
$$

2.3.2. Equivalent shear modulus

The equivalent shear modulus of a fiber reinforced orthotropic element can be defined as in the Eq. (8) depending on the material properties [14].

$$G_{eq} = \frac{1}{h\,A_{55}^{*}} \tag{8}$$

In this equation A_{55}^{*} can be calculated from;

$$
\begin{aligned}
&A_{55}^{*} = \frac{A_{44}}{(A_{44}A_{55} - A_{45}A_{45})}, \qquad A_{ij} = h\overline{Q}_{ij} \\
&\overline{Q}_{44} = Q_{44}\cos^2\theta + Q_{55}\sin^2\theta, \qquad \overline{Q}_{45} = (Q_{55} - Q_{44})\sin\theta\cos\theta \\
&\overline{Q}_{55} = Q_{44}\sin^2\theta + Q_{55}\cos^2\theta, \qquad Q_{44} = G_{23}, \qquad Q_{55} = G_{13}
\end{aligned} \tag{9}
$$

angles of the fibers.

2. Theoretical Formulation

In this study, two beams are investigated with different loading and boundary conditions. As can be seen from Figure 4; the first one is a cantilever beam loaded by a vertical single load applied at the free tip. The second one is a simply supported beam with a uniformly distributed load.

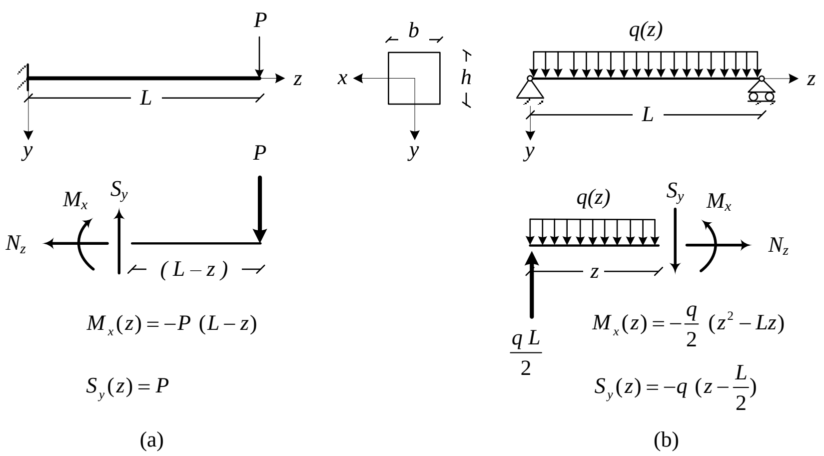

Figure 4. Internal forces in orthotropic beam examples; (a) Cantilever beam (b) Simply supported beam

3.1. Cantilever Beam Solution Based on EBT

Moment-curvature relationship for the orthotropic prismatic cantilever beams of length L and has constant flexural rigidity as given in Figure 4a is according to the EBT as follows;

$$\frac{\partial^2 u_{y1}}{\partial z^2} = -\frac{M_x(z)}{E_{eq}\, I_x} = \frac{1}{E_{eq}\, I_x}(-P\,z + P\,L) \tag{10}$$

Boundary conditions for this beam are as follows;

$$\left.\frac{\partial u_{y1}}{\partial z}\right|_{z=0} = 0 \;, \qquad \left.u_{y1}\right|_{z=0} = 0 \tag{11}$$

Deflection formula along the axis of the orthotropic cantilever beam is obtained as;

$$u_{y1} = \frac{1}{E_{eq} I_x}\left(-\frac{P}{6} z^3 + \frac{PL}{2} z^2\right) \tag{12}$$

Maximum deflection occurs at the tip of the beam and its value is;

$$\left.u_{y1}\right|_{z=L} = \frac{PL^3}{3E_{eq} I_x} \tag{13}$$

3.2. Simply Supported Beam Solution Based on EBT

Moment-curvature relationship for the orthotropic prismatic simply supported beam of length L and has constant flexural rigidity as given in Figure 4b is according to the EBT as;

$$\frac{\partial^2 u_{y1}}{\partial z^2} = -\frac{M_x(z)}{E_{eq}\, I_x} = \frac{1}{E_{eq}\, I_x}\left(-\frac{q}{2} z^2 + \frac{q\,L}{2} z\right) \tag{14}$$

This beam satisfies the boundary conditions of,

$$\left.u_{y1}\right|_{z=0} = 0 \;, \quad \left.u_{y1}\right|_{z=L} = 0 \tag{15}$$

Deflection formula of a point along the axis of the orthotropic simply supported beam is,

$$u_{y1} = \frac{q}{E_{eq}\, I_x}\left(\frac{1}{24} z^4 - \frac{L}{12} z^3 + \frac{L^3}{24} z\right) \tag{16}$$

Maximum deflection occurs at the midlength of the beam. Calculated value of the maximum deflection is,

$$\left.u_{y1}\right|_{z=L/2} = \frac{5\,q\,L^4}{384\,E_{eq}\, I_x} \tag{17}$$

3.3. Cantilever Beam Solution Based On TBT

As an example, in the case of the orthotropic cantilever beam of length L and has constant flexural rigidity as given in Figure 4a, rotation of a point along the axis of the beam can be calculated according to the TBT as [12],

$$\frac{\partial u_{y1}}{\partial z} = -\frac{S_y(z)}{\kappa G_{eq} A_{xy}} - \phi_x \tag{18}$$

The κ in this equation is the shear correction factor that depends on the geometry of the cross section. Boundary conditions for this beam are as follows;

$$\left.\frac{\partial u_{y1}}{\partial z}\right|_{z=0} = 0 \ , \qquad u_{y1}\big|_{z=0} = 0 \tag{19}$$

Deflection for the orthotropic prismatic cantilever beam of length L as given in Figure 4a can be calculated according to the TBT as follows [12];

$$u_{y1} = \frac{1}{E_{eq} I_x}\left(-\frac{P}{6} z^3 + \frac{PL}{2} z^2\right) + \frac{1}{\kappa G_{eq} A_{xy}}(Pz) \tag{20}$$

If $z = L$ is substituted into Eq. (20), maximum deflection value is obtained as,

$$u_{y1}\big|_{z=L} = \frac{PL^3}{3E_{eq} I_x} + \frac{PL}{\kappa G_{eq} A_{xy}} \tag{21}$$

3.4. Simply Supported Beam Solution Based on TBT

For example, in the case of the orthotropic simply supported beam which carries a uniformly distributed load of intensity q and has constant flexural rigidity, rotation of a point along the axis of the beam can be calculated according to the TBT as,

$$\frac{\partial u_{y1}}{\partial z} = -\frac{S_y(z)}{\kappa G_{eq} A_{xy}} - \phi_x \tag{22}$$

Boundary conditions for prismatic orthotropic simply supported beams loaded with uniformly distributed load are,

$$u_{y1}\big|_{z=0} = 0 \ , \quad u_{y1}\big|_{z=L} = 0 \ , \quad \left.\frac{\partial u_{y1}}{\partial z}\right|_{z=L/2} = 0 \tag{23}$$

Deflection formula of a point along the axis of the orthotropic simply supported beam is,

$$u_{y1} = \frac{q}{E_{eq} I_x}\left(\frac{1}{24} z^4 - \frac{L}{12} z^3 + \frac{L^3}{24} z\right) + \frac{q}{\kappa G_{eq} A_{xy}}\left(-\frac{1}{2} z^2 + \frac{L}{2} z\right) \tag{24}$$

Maximum deflection occurs at the midlength of the beam and its value is,

$$u_{y1}\big|_{z=L/2} = \frac{5}{384}\frac{qL^4}{E_{eq} I_x} + \frac{q}{\kappa G_{eq} A_{xy}}\left(\frac{L^2}{8}\right) \tag{25}$$

4. Numerical Results

In this study, two orthotropic beam examples are solved according to EBT and TBT. In these examples different orthotropic materials are used and the results are presented in tables and graphs. By using equivalent moduli orthotrophic beams are modeled as if isotropic beams. The results obtained by using isotropic steel material and the results obtained by using orthotropic materials are also compared. The mechanical properties of the materials used in the examples are given in Table 1 [13-15].

Table 1. Mechanical properties of materials used in the examples

	Graphite– Epoxy	Glass – Epoxy	Boron – Epoxy	Steel
E_1	137.90 GPa	53.78 GPa	206.85 GPa	206.182 GPa
E_2	8.96 GPa	17.93 GPa	20.69 GPa	206.182 GPa
v_{12}	0.3	0.25	0.3	0.29
G_{12}	7.10 GPa	8.96 GPa	6.90 GPa	79.434 GPa
G_{13}	7.10 GPa	8.96 GPa	6.90 GPa	79.434 GPa
G_{23}	6.21 GPa	3.45 GPa	4.14 GPa	79.434 GPa

The geometry of the orthotropic beam as given in Figure 1 has a unit cross sectional area and its cross sectional dimensions are taken as $b=1, h=1.$ The length of the example beam is taken as $L_1=10, L_2=20$ and $L_3=100$ respectively [14]. A unit vertical load of $P=1$ is applied at the tip of the orthotropic cantilever beam. For the orthotropic simply supported beam, intensity of the applied uniformly distributed load is $q=1.$ The maximum deflection values of orthotropic beams are calculated by carrying out static analysis based on different beam theories. Firstly; equivalent Young's modulus depending on material properties, is calculated using Eq. (5). For static analysis of orthotropic beams according to the TBT also equivalent shear modulus is needed. Equivalent shear modulus, depending on the material properties are calculated using Eq. (8). Calculated equivalent modulus are given in Table 2. The values on the left in Table 2 represent equivalent Young's moduli and the values on the right represent equivalent shear moduli.

Table 2. Equivalent Young's / Shear Moduli of the materials

θ	Graphite – Epoxy (GPa)	Glass – Epoxy (GPa)	Boron – Epoxy (GPa)	Steel (GPa)
0^0	137.90 / 7.10	53.78 / 8.96	206.85 / 6.90	206.18 / 79.43
30^0	27.29 / 6.85	30.19 / 6.40	30.89 / 5.91	206.18 / 79.43
45^0	15.67 / 6.63	22.64 / 4.98	20.49 / 5.18	206.18 / 79.43
60^0	11.26 / 6.41	19.34 / 4.08	18.48 / 4.60	206.18 / 79.43
90^0	8.96 / 6.21	17.93 / 3.45	20.69 / 4.14	206.18 / 79.43

When the moment of inertia of the related beams is calculated by the equation $I_x = bh^3/12 = 1\times 1^3/12$ then $I_x = 1/12.$ In this case, according to the EBT, the maximum deflections can be calculated for the cantilever beam and for the simply supported beam respectively as,

$$
\begin{aligned}
u_{y1}\big|_{z=L} &= \frac{PL^3}{3E_{eq}I_x} = \frac{1\times L_i^{\,3}}{3E_{eq}(1/12)} = 4\times\frac{L_i^{\,3}}{E_{eq}} \\
u_{y1}\big|_{z=L/2} &= \frac{5\,q\,L^4}{384\,E_{eq}I_x} = \frac{5\times 1\times L_i^{\,4}}{384\,E_{eq}(1/12)} = \frac{5}{32}\times\frac{L_i^{\,4}}{E_{eq}}
\end{aligned}
\tag{26}
$$

The deflections are put in a dimensionless form by using Eq. (27) for the cantilever beam and simply supported beam respectively as;

$$\hat{u}_{y1} = u_{y1} \times \frac{E_2 \times b \times h^3}{P \times L^3} \times 100$$
$$\hat{u}_{y1} = u_{y1} \times \frac{E_2 \times b \times h^3}{q \times L^4} \times 100 \tag{27}$$

Using the values given in Table 2, the maximum deflection values for the cantilever beam according to EBT are calculated and given in Table 3a.

Table 3a. Maximum dimensionless deflection values along the axis of the cantilever beam according to the EBT.

θ	Graphite – Epoxy	Glass – Epoxy	Boron – Epoxy	Steel
0^0	25.990	133.358	40.010	400.000
30^0	131.343	237.595	267.896	400.000
45^0	228.796	316.781	403.856	400.000
60^0	318.348	370.916	447.891	400.000
90^0	400.000	400.000	400.000	400.000

The maximum deflection values for the simply supported beam according to EBT are calculated and given in Table 3b.

Table 3b. Maximum dimensionless deflection values along the axis of the simply supported beam according to the EBT.

θ	Graphite – Epoxy	Glass – Epoxy	Boron – Epoxy	Steel
0^0	1.015	5.209	1.563	15.625
30^0	5.131	9.281	10.465	15.625
45^0	8.937	12.374	15.776	15.625
60^0	12.436	14.489	17.496	15.625
90^0	15.625	15.625	15.625	15.625

Since the example cantilever beam has a rectangular cross section, its shear correction factor is $\kappa = 5/6$. Cross sectional area is $A = 1 \times 1 = 1$. In this case, according to the TBT, the maximum deflections can be calculated for the cantilever beam and for the simply supported beam respectively as,

$$u_{y1}\Big|_{z=L} = \frac{PL^3}{3E_{eq}I_x} + \frac{\alpha PL}{G_{eq}A_{xy}} = \frac{1 \times L_i^3}{3E_{eq}(1/12)} + \frac{1,2 \times 1 \times L_i}{G_{eq}(1)} = (4 \times \frac{L_i^3}{E_{eq}}) + (1,2 \times \frac{L_i}{G_{eq}})$$
$$u_{y1}\Big|_{z=L/2} = \frac{5\,q\,L^4}{384\,E_{eq}I_x} + \frac{\alpha\,q\,L^2}{8G_{eq}A_{xy}} = \frac{5 \times 1 \times L_i^4}{384\,E_{eq}(1/12)} + \frac{1,2 \times 1 \times L_i^2}{8G_{eq}(1)} = \frac{5}{32} \times \frac{L_i^4}{E_{eq}} + \frac{1,2}{8} \times \frac{L_i^2}{G_{eq}} \tag{28}$$

Using the values given in Table 2, the maximum deflection values at the tip of the cantilever beam according to the TBT are calculated and are given in Table 4a. The length / depth ratio (L/h) for each composite material is calculated for 10, 20 and 100, respectively.

Table 4a. Maximum dimensionless deflection values along the axis of the cantilever beam according to the TBT.

Material	L/h	θ				
		0^0	30^0	45^0	60^0	90^0
Graphite – Epoxy	10	27.504	132.912	230.419	320.026	401.731
	20	26.368	131.735	229.202	318.768	400.433
	100	26.005	131.359	228.812	318.365	400.017
Glass – Epoxy	10	135.759	240.955	321.100	376.194	406.237
	20	133.958	238.435	317.861	372.236	401.559
	100	133.382	237.629	316.825	370.969	400.062
Boron – Epoxy	10	43.608	272.094	408.654	453.288	405.997
	20	40.909	268.945	405.055	449.240	401.499
	100	40.046	267.938	403.904	447.945	400.060
Steel	10	403.115	403.115	403.115	403.115	403.115
	20	400.779	400.779	400.779	400.779	400.779
	100	400.000	400.000	400.000	400.000	400.000

The maximum deflection values for the simply supported beam according to TBT are calculated and given in Table 4b.

Table 4b. Maximum dimensionless deflection values along the axis of the simply supported beam according to the TBT

Material	L/h	θ				
		0^0	30^0	45^0	60^0	90^0
Graphite – Epoxy	10	1.205	5.327	9.140	12.645	15.841
	20	1.063	5.180	8.988	12.488	15.679
	100	1.017	5.133	8.939	12.438	15.627
Glass – Epoxy	10	5.509	9.701	12.914	15.149	16.405
	20	5.284	9.386	12.509	14.654	15.820
	100	5.212	9.285	12.380	14.496	15.633
Boron – Epoxy	10	2.013	10.989	16.375	18.170	16.375
	20	1.675	10.596	15.926	17.664	15.812
	100	1.567	10.470	15.782	17.503	15.633
Steel	10	16.014	16.014	16.014	16.014	16.014
	20	15.722	15.722	15.722	15.722	15.722
	100	15.629	15.629	15.629	15.629	15.629

Maximum dimensionless deflection values along the axis of the cantilever beam by using Table 3a and Table 4a are given graphically in Figure 5.

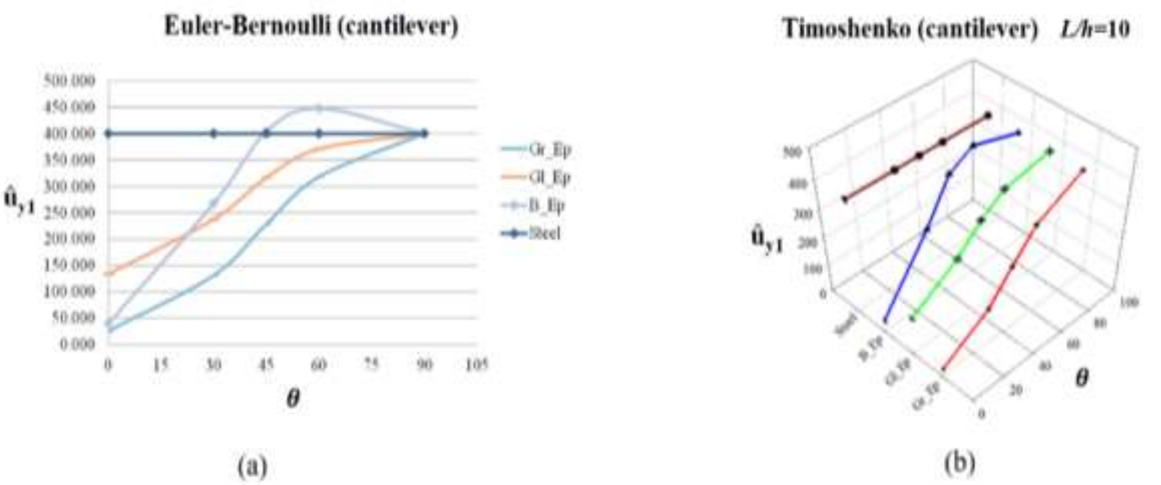

Figure 5. Maximum dimensionless deflection values of the cantilever beam (a) according to EBT (b) according to TBT.

Maximum dimensionless deflection values along the axis of the simply supported beam by using Table 3b and Table 4b are given graphically in Figure 6.

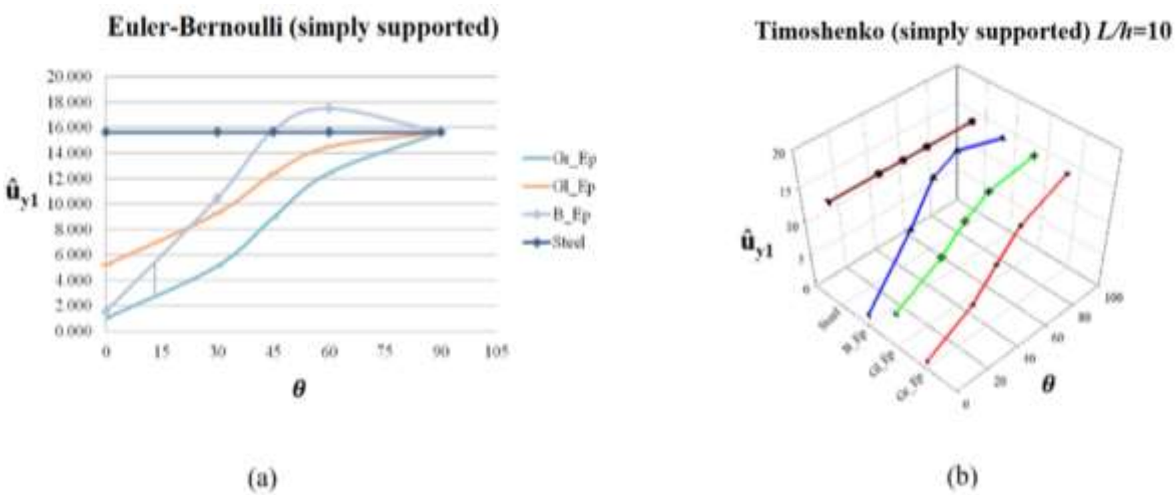

Figure 6. Maximum dimensionless deflection values of the simply supported beam (a) according to EBT (b) according to TBT.

Deflections for a simply supported and a cantilever orthotropic beam for orientation angles of $\theta = 0^{\circ}$ and $\theta = 60^{\circ}$ with $L = 20$ is given in Figure 7.

When the orientation angle θ increases deflection values for orthotropic beams also increases as seen in Figure 7. Also deflection values for orthotropic beams with TBT are greater than EBT. It could be easily seen from Figure 7; deflection values for isotropic beam produced from steel material are greater than orthotropic beams produced from composite materials for $\theta = 0^{\circ}$. When the orientation angle $\theta = 60^{\circ}$, beams produced with Boron-Epoxy composite material has the maximum deflection value and beams produced with Graphite Epoxy composite material has the minimum displacement value.

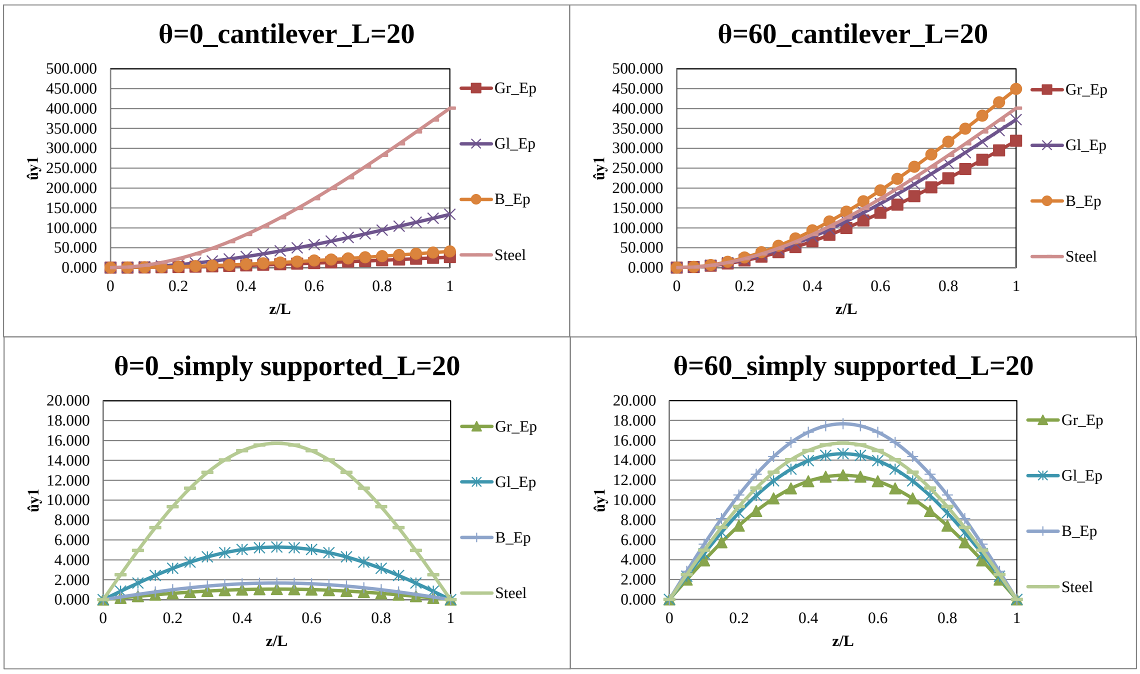

Figure 7. Displacements for simply supported and cantilever orthotropic beams for orientation angle $\theta = 0^{o}$ and $\theta = 60^{o}$ with $L = 20$ according to Timoshenko Beam Theory

4.1. Verification

The suitability of the presented approach (isotropic solution using the Equivalent Module) has been verified by comparing the solution of one case with finite element analysis software ANSYS.

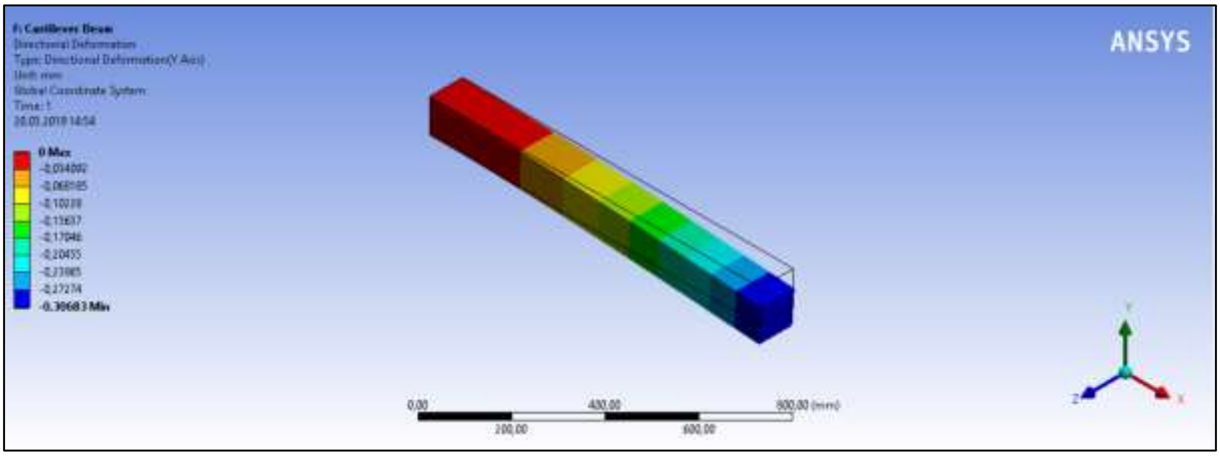

Figure 8. ANSYS solution for cantilever Graphite-Epoxy beam for orientation angle $\theta = 0^{o}$ with $L/h = 10$

In ANSYS program, discussed sample is modeled as orthotropic Graphite-Epoxy material as seen in Figure 8. Cross sectional dimensions of the cantilever beam are taken as $b = 100$ mm, $h = 100$ mm. The length of the example beam is taken as $L_1 = 1000$ mm, $L_2 = 2000$ mm and $L_3 = 10000$ mm respectively. A vertical load of $P = 1000$ N is applied at the tip of the orthotropic cantilever beam. After calculating the maximum deflection values along the axis of the cantilever beam according to the EBT, the deflections are put in a dimensionless form by using Eq. (27). Dimensionless deflection calculation results for $L/h = 10$ is 27.492, for $L/h = 20$ is 26.358 and for $L/h = 100$ is 26.001. Fair agreement was obtained between the results calculated from this study and ANSYS software.

5. Conclusion

In this study, by developing computer programs orthotropic beams are analysed statically according to EBT and TBT. According to the EBT and TBT, the deflection values of the orthotropic beam are calculated and presented in the form of tables and graphs.

Equivalent Young's modulus and equivalent shear modulus values are calculated since the mechanical properties of orthotropic material, such as Young's modulus and shear modulus, changes depending on the direction. By using these calculated values, a static analysis of a cantilever beam loaded by a vertical force applied at the free tip and a simply supported beam with a uniformly distributed load is performed. In the analysis, three different orthotropic materials and an isotropic steel material, namely graphite-epoxy, glass-epoxy, boron-epoxy and steel are considered. Calculations are made for different orientation angles of these materials.

The problems are considered separately according to the EBT and the TBT. In the calculations made according to the EBT, it is seen that the dimensionless maximum deflection value increases as the orientation angle in the orthotropic composite cantilever beam increases. If the orientation angle is 0^0 the fibers are parallel to the beam axis. In this case, the values of dimensionless deflection values are almost the same for all but glass-epoxy material. For glass-epoxy material this has a greater value. The authors believe that this is due to the fact that the E_1 value of the glass-epoxy material is lower than the others. If the angle of orientation is 90^0 the fibers are perpendicular to the axis of the beam, and all materials have the same dimensionless deflection value. This value is the maximum dimensionless deflection value for non-boron-epoxy materials. For the boron-epoxy material, the maximum dimensionless value of deflection is obtained at the angle of orientation of 60^0.

In the calculations made according to the TBT, it is seen that as the orientation angle increases, the maximum dimensionless deflection value also increases. For the four different materials, calculations are made separately for the length / depth ratio (L/h) of 10, 20 and 100 respectively. For the materials, in the case of fibers parallel to the beam axis, the values of the dimensionless deflection values are almost the same except for the glass-epoxy material. When the fibers are perpendicular to the beam axis, the dimensionless deflection values of all materials are approximately the same. As the length / depth ratio decreases, the dimensionless deflection values increase. Thus the difference between the deflection results obtained from TBT and EBT are more significant. In this study, an orthotropic cantilever and simply supported beam with different materials are treated and the results are examined. Analyses can also be made using beams with other boundary conditions and different materials.

References

[1] Labuschange A., van Rensburg N.F.J., van der Merwe A.J. 2009. Comparison of linear beam theories. Mathematical and Computer Modelling, 49: 20-30.

[2] Reddy J.N. 2010. Nonlocal nonlinear formulations for bending of classical and shear deformation theories of beams and plates. International Journal of Engineering Science, 48: 1507–1518.

[3] Sayyad A.S. 2011. Comparison of various refined beam theories for the bending and free vibration analysis of thick beams. Applied and Computational Mechanics, 5: 217–230.

[4] Aykanat B.A. 2007. Investigation of a Cantilevered Bar Subjected to Uniformly Distributed Force in Nonlocal Elasticity. Master Thesis, Istanbul Technical University, Graduate School of Science Engineering and Technology, 29pp, Istanbul.

[5] Carrera E., Giunta G. 2010. Refined beam theories based on a unified formulation. International Journal of Applied Mechanics, 2: 117–143.

[6] Elshafei M.A. 2013. FE modeling and analysis of isotropic and orthotropic beams using first order shear deformation theory. Materials Sciences and Applications, 4: 77–102.

[7] Whitney J.M. 1985. Elasticity analysis of orthotropic beams under concentrated loads. Composites Science and Technology, 22: 167–184.

[8] Li X.F. 2008. A unified approach for analyzing static and dynamic behaviors of functionally graded Timoshenko and Euler–Bernoulli beams. Journal of Sound and Vibration, 318: 1210–1229.

[9] De Rosa M.A., Franciosi C. 2013. A simple approach to detect the nonlocal effects in the static analysis of euler-bernoulli and timoshenko beams. Mechanics Research Communications, 48: 66-69.

[10] Palmeri A., Cicirello, A. 2011 Physically-based dirac's delta functions in the static analysis of multi-cracked euler-bernoulli and timoshenko beams. International Journal of Solids and Structures, 48 (14-15), 2184-2195

[11] Saraçoğlu M.H., Güçlü G. Uslu F. 2017 Static analysis of orthotropic beams by different beam theories. in Proc. 20th National Mechanical Congress pp 351-361 05-09 September 2017 Bursa.

[12] Carrera E., Giunta G., Petrolo M. 2011. Beam Structures: Classical and Advanced Theories 1st ed., John Wiley & Sons, New Delhi, India.

[13] Haque A. 2016 http://www.clearlyimpossible.com/ahaque/timoshenko.pdf (Date of access: 30.01.2018)

[14] Reddy J.N. 2004. Mechanics of Laminated Composite Plates and Shells: theory and analysis 2nd ed., CRC Press, Florida, USA.

[15] Jones R.M. 1999. Mechanics of Composite Materials 2nd ed., Taylor & Francis, Philadelphia, USA.